



UDC 541.123.3

PHASE EQUILIBRIA IN THE La_2O_3 - Lu_2O_3 - Er_2O_3 SYSTEM AT 1500 AND 1600 °C

Olga V. Chudinovych^{1,2}, Olexandr V. Shyrokov¹, Anatoly V. Samelyuk¹¹ Frantsevich Institute for Materials Science Problems NASU, Krzhizhanovsky, 3str., Kyiv, 03142, Ukraine² National Technical University of Ukraine «Igor Sikorsky Kyiv Polytechnic Institute», 37 Pobedy Ave., Kyiv, 03056, Ukraine

Received 9 January 2023; accepted 7 February 2023; available online 25 April 2023

Abstract

The phase relations in the La_2O_3 - Lu_2O_3 - Er_2O_3 ternary system at 1500 and 1600 °C were studied in the whole concentration range by X-ray diffraction (XRD) and scanning electron microscopy (SEM). Oxides of La, Lu, and Er (99.99 %) were used as starting substances. The samples were prepared with a concentration step of 1-5 mol. %. The oxides were dissolved in HNO_3 (1:1) followed by evaporation of the solutions and decomposition of nitrates at 800 °C for 2 hours. The samples were heat treated at 1500 °C (for 70 h), and 1600 °C (for 10 h) in air. The phase composition of the test samples studied by X-ray diffraction (XRD, DRON-3), microstructural phase and electron microprobe X-ray (Superprobe-733, JEOL, Japan, Palo Alto, CA) analyses. Solid solutions based on various polymorphic forms of original oxides and ordered LaLuO_3 (LaErO_3) phases were detected in the system. No new phases were found in the system. The isothermal cross-sections of the La_2O_3 - Lu_2O_3 - Er_2O_3 phase diagram at 1500 and 1600 °C are characterized by the presence of three single-phase (A- La_2O_3 , R, C- Lu_2O_3 (Er_2O_3)) and two two-phase (C+R, A+R) regions. The system forms continuous series of solid solutions based on the cubic modification of C- Lu_2O_3 (Er_2O_3) and the ordered perovskite-type phase (R-phase). Solubility limits are determined and concentration dependences of periods also lattice parameters of the unit cell of phases formed in the system are constructed. The range of homogeneity of solid solutions based on the R-phase extends from 46 to 54 mol % La_2O_3 at 1500 °C and from ~48 to 54 mol % La_2O_3 at 1600 °C. Lutetium and erbium oxides form an continuous series of C-REE oxide solid solutions.

Keywords: phase equilibria; lanthana; Lutetia; erbia; lattice parameters.

ФАЗОВІ РІВНОВАГИ В СИСТЕМІ La_2O_3 - Lu_2O_3 - Er_2O_3 ЗА 1500 І 1600 °C

Ольга В. Чудінович^{1,2}, Олександр В. Широков¹, Анатолій В. Самелюк¹¹ Інститут проблем матеріалознавства ім. І.М. Францевича НАН України, м. Київ² Національний технічний університет України «Київський політехнічний інститут імені Ігоря Сікорського», м. Київ

Анотація

Фазові співвідношення в потрійній системі La_2O_3 - Lu_2O_3 - Er_2O_3 за 1500 і 1600 °C вивчали в усьому діапазоні концентрацій методами рентгенівської дифракції (РФА) і скануючої електронної мікроскопії (СЕМ). Як вихідні речовини використовували оксиди La, Lu та Er (99.99 %). Зразки готували з кроком концентрування 1-5 мол. %. Оксиди розчиняли в HNO_3 (1 : 1) з наступним випарюванням розчинів і розкладанням нітратів за 800 °C протягом 2 годин. Зразки піддавали термічній обробці за 1500 °C (протягом 70 годин) та 1600 °C (протягом 10 годин) на повітрі. Фазовий склад досліджуваних зразків вивчали за допомогою рентгенофазового (РФА, ДРОН-3), мікроструктурного та електронно-мікронного (Superprobe-733, JEOL, Японія, Пало-Альто, Каліфорнія) аналізів. У системі виявлено тверді розчини на основі різних поліморфних форм вихідних оксидів і впорядкованих фаз LaLuO_3 (LaErO_3). Нових фаз у системі не виявлено. Ізотермічні перерізи фазової діаграми стану La_2O_3 - Lu_2O_3 - Er_2O_3 при 1500 і 1600 °C характеризуються наявністю трьох однофазних (A- La_2O_3 , R, C- Lu_2O_3 (Er_2O_3)) і двох двофазних (C+R, A+R) областей. Система утворює безперервну серію твердих розчинів на основі кубічної модифікації C- Lu_2O_3 (Er_2O_3) та впорядкованої фази типу перовскіту (R-фаза). Визначено межі розчинності та побудовано концентраційні залежності періодів і параметрів ґратки елементарної комірки фаз, що утворюються в системі. Діапазон гомогенності твердих розчинів на основі R-фази простягається від 46 до 54 мол. % La_2O_3 за 1500 °C і від ~48 до 54 мол. % La_2O_3 за 1600 °C. Оксиди лютецію та ербію утворюють неперервний ряд твердих розчинів оксидів C-REE.

Ключові слова: фазові рівноваги, лантан, лютецій, ербій, параметри ґратки.

*Corresponding author: e-mail address: e-mail: chudinovych_olia@ukr.net

© 2023 Oles Honchar Dnipro National University;

doi: 10.15421/jchemtech.v31i1.271493

Introduction

The phosphors based on lanthanides oxides represent a perspective class of materials for photovoltaic devices [1–6]. Materials based on solid solutions of rare earth element (REE) oxides are used in radio electronics, optoelectronics, instrument engineering, nuclear and laser engineering, mechanical engineering, the chemical industry, metallurgy, medicine, etc. REE compounds are used to create laser and other optically active elements [6]. Doping lanthanum oxide with different REE allows for obtaining substances with special optical, luminescent, and dielectric properties, which makes it attractive as a material for photo converters. Lu_2O_3 has a high density, which is important for scintillation materials [7]. Lanthanum oxide is a part of high-tech glasses for special purpose, transmitting infrared and absorbing ultraviolet rays [8–10].

The phase equilibria in the La_2O_3 – Lu_2O_3 system were examined by X-ray diffraction and thermal analysis at high temperatures [11]. The melt was crystallized at temperatures above 2000 °C to obtain perovskite-like LaLuO_3 single crystals. The orthorhombic cell parameters are $a = 6.00$ nm, $b = 5.79$ nm, $c = 8.35$ nm and space group is Pnam [11]. The paper [12] provides calculations of oxygen vacancies in La_2O_3 , Lu_2O_3 , and LaLuO_3 but there was no data on phase equilibria.

The La_2O_3 – Lu_2O_3 system at 1500 °C (and at 1600 °C) is characterized by the hexagonal (A) modification of lanthanum oxide with the solubility of Lu_2O_3 9 mol.% (and 9 mol.% at 1600 °C), cubic (C) modification of lutetium oxide with the solubility of A- La_2O_3 4 mol.% (and 7 mol. % at 1600 °C), and ordered perovskite-type LaLuO_3 (R) phase in the range 48–56 mol.% Lu_2O_3 (and 48–55 mol.% Lu_2O_3 at 1600 °C) [13].

The phase relations and structures of the phases formed in the La_2O_3 – Er_2O_3 system are examined in [11, 14–21]. It should be noted that this system was studied experimentally [21] and assessed thermodynamically [18]. According to X-ray diffraction, an ordered LaErO_3 (R) perovskite-type phase with a narrow homogeneity range forms in the La_2O_3 – Er_2O_3 system [11]. The lattice parameters of the unit cell in the ordered stoichiometric LaErO_3 phase are as follows: $a = 0.5864$ nm, $b = 0.6082$ nm, and $c = 0.8466$ nm. The compound remains stable up to 1800 °C then transforms into a hexagonal H- La_2O_3 solid solution [17]. In the above system, there are solid solutions of cubic (C) and hexagonal (H) Er_2O_3 modifications and low-

temperature hexagonal (A) and high-temperature hexagonal (H) and cubic (X) La_2O_3 modifications.

The La_2O_3 – Er_2O_3 system at 1100 °C (and at 1500 °C) is characterized by the hexagonal (A) modification of lanthanum oxide with the solubility of Er_2O_3 5 mol.% (and 13 mol. % at 1500 °C), cubic (C) modification of erbium oxide with the solubility of A- La_2O_3 ~6 mol.% (and ~11 mol. % at 1500 °C), and ordered perovskite-type LaErO_3 (R) phase in the range 45–51 mol.% Er_2O_3 (and 45–51 mol.% Er_2O_3 at 1500 °C) [14].

The phase diagrams of the system consisted of oxides at the end of the lanthanide series feature infinite solid solutions based on A, B, C, H, and X modifications of REE oxides [18; 20, 22–25].

Phase equilibria in binary systems based on oxides of rare earth elements have been studied completely [11–25]. Information on phase equilibria in the ternary La_2O_3 – Lu_2O_3 – Er_2O_3 system is absent and requires further research. The purpose of this work is to study the interaction of lanthanum, lutetium and erbium oxides at 1500 and 1600 °C in the whole concentration range and to construct the corresponding isothermal cross-section of the phase diagram.

Experimental

The starting materials were Lu_2O_3 , La_2O_3 , and Er_2O_3 (produced by «Merck» Corp.) with 99.99 % of the main component. The samples were prepared with a concentration step of 1–5 mol. %. Weighed oxide portions were dissolved in HNO_3 (1:1) and then the solutions were evaporated and the nitrates decomposed into oxides by calcination at 800 °C for 2 h. The powders were pressed as pellets 5 mm in diameter and 4 mm in height at 10 MPa. The samples were heat treated in three stages: in a furnace with H23U5T (FeCrAl alloy) heating elements at 1100 °C and with molybdenum disilicide (MoSi_2) heating elements at 1500 °C (70 h) and 1600 °C (10 h) in air.

The samples were subjected to X-ray powder diffraction using a DRON-3 diffractometer at room temperature (Cu- $K\alpha$ radiation). The scan angle was 0.05–0.1 ° in the range $2\theta = 15$ –90 °. The lattice parameters were calculated with the least-square method employing the LATTIC software [26], with an error of less than 0.0002 nm for the cubic phase. The phase composition was determined of the Joint Committee on Powder Diffraction Standards (JCPDS International Center for Diffraction Data, 1999).

The microstructures of the samples were studied by scanning electron microscopy with a

Superprobe-733 analyzer (JEOL, Japan) in back-scattered electrons (BSE) and secondary electrons (SE).

Results and Discussion

For the study samples were taken, the compositions of which lie on two beams Lu_2O_3 -

(50 mol % La_2O_3 -50 mol % Er_2O_3) and La_2O_3 -(50 mol % Lu_2O_3 -50 mol % Er_2O_3).

The chemical and phase composition of the samples annealed at 1500 and 1600°C and the lattice parameters of the phases in equilibrium at these temperatures are summarized in Tables 1 and 2, respectively.

Table 1

Phase composition and lattice parameters of the phases in the La_2O_3 - Lu_2O_3 - Er_2O_3 samples, annealed at 1500 °C for 70 h

Chemical composition (mol %)			Phases by XRD	Lattice parameters of the phases $\sigma \pm 0.0002$ (nm)					
Lu_2O_3	La_2O_3	Er_2O_3		R		<C>		<A>*	
				<i>a</i>	<i>b</i>	<i>c</i>	<i>a</i>	<i>a</i>	<i>c</i>
Section Lu_2O_3 —(50 mol % La_2O_3 —50 mol % Er_2O_3)									
0	50	50	R	0.612	0.588	0.840			
1	49.5	49.5	R	0.609	0.585	0.842			
2	49	49	R+<C>tr.	0.586	0.583	0.851			
3	48.5	48.5	R+<C>	0.606	0.585	0.842	1.052		
4	48	48	R+ <C>	0.594	0.584	0.852	1.041		
5	47.5	47.5	R+ <C>				1.047		
10	45	45	R + <C>	0.583	0.583	0.857	1.045		
15	42.5	42.5	R + <C>	0.598	0.584	0.850	1.036		
20	40	40	R + <C>	0.609	0.581	0.833	1.049		
30	35	35	R + <C>	0.548	0.583	0.875	1.047		
70	15	15	R + <C>	0.603	0.582	0.836	1.042		
80	10	10	Rtr. + <C>				1.042		
85	7.5	7.5	Rtr.+ <C>				1.041		
90	5	5	Rtr. + <C>				1.040		
95	2.5	2.5	<C>	—	—	—	1.039		
100	0	0	<C>	—	—	—	1.039		
Section La_2O_3 —(50 mol % Lu_2O_3 —50 mol % Er_2O_3)									
50	0	50	<C>				1.044		
49	2	49	<C>				1.047		
48	4	48	<C>				1.047		
47.5	5	47.5	<C>				1.048		
45	10	45	Rtr. + <C>				1.049		
30	40	30	R + <C>	0.549	0.583	0.874	1.049		
29	42	29	R + <C>	0.605	0.583	0.838	1.049		
27.5	45	27.5	R + <C>	0.607	0.584	0.841			
26	48	26	R	0.594	0.582	0.846			
25	50	25	R	0.596	0.582	0.848			
23.5	53	23.5	R	0.603	0.582	0.857			
22.5	55	22.5	<A> + R	0.603	0.583	0.860		0.650	0.393
20	60	20	<A> + R	0.598	0.585	0.860		0.654	0.385
7.5	85	7.5	<A> + R	0.610	0.584	0.861		0.652	0.379
5	90	5	<A> + Rtr.	0.568	0.581	0.866		0.650	0.384
4	92	4	<A> + Rtr.					0.650	0.386
2.5	95	2.5	<A>					0.651	0.387

*) Note that the oxide of lanthanum is subject to hydration in air and, thus, instead of hexagonal A- La_2O_3 in the samples after heat treatment at 1500 °C we found the formation of hexagonal A- $\text{La}(\text{OH})_3$. This arose in this work, however, proper storage and prompt investigation after annealing would have made it possible to obtain A- La_2O_3 . Nevertheless, since this applies only to A- La_2O_3 in the investigated system, the results obtained for $\text{La}(\text{OH})_3$ can be attributed to A- La_2O_3 . Designation of phases: <A> - solid solutions based on hexagonal modifications of $\text{La}(\text{OH})_3$; <C> - solid solutions based on cubic modification of $\text{Lu}_2\text{O}_3(\text{Er}_2\text{O}_3)$; R - ordered phase of $\text{LaLuO}_3(\text{LaErO}_3)$ with perovskite-type structure with rhombic distortions.

Phase composition and lattice parameters of the phases in the La₂O₃-Lu₂O₃-Er₂O₃ samples, annealed at 1600 °C for 10 h

Chemical composition (mol %)			Phases by XRD	Lattice parameters of the phases $\sigma \pm 0.0002$ (nm)						
Lu ₂ O ₃	La ₂ O ₃	Er ₂ O ₃		R			<C>		<A>*	
				a	b	c	a	a	c	
Section Lu ₂ O ₃ —(50 mol % La ₂ O ₃ —50 mol % Er ₂ O ₃)										
0	50	50	R							
1	49.5	49.5	R	0.6043	0.5842	0.8444				
2	49	49	R+<C>tr.	0.6039	0.5813	0.8419				
3	48.5	48.5	R+<C>							
4	48	48	R+ <C>	0.6045	0.5838	0.8435				
5	47.5	47.5	R+ <C>	0.6038	0.5843	0.8425	1.0466			
10	45	45	R + <C>							
15	42.5	42.5	R + <C>	0.6027	0.5837	0.8428				
20	40	40	R + <C>	0.6024	0.5828	0.8411	1.0534			
30	35	35	R + <C>	0.6002	0.5821	0.8407	1.0458			
70	15	15	R + <C>	0.5971	0.5828	0.8355	1.0419			
80	10	10	R+ <C>	0.6013	0.5790	0.8382	1.0415			
85	7.5	7.5	R tr+ <C>	0.607	0.583	0.8274	1.0421			
90	5	5	R tr. + <C>				1.040			
95	2.5	2.5	<C>	—	—	—	1.0389			
100	0	0	<C>	—	—	—	1.039			
Section La ₂ O ₃ —(50 mol % Lu ₂ O ₃ —50 mol % Er ₂ O ₃)										
50	0	50	<C>				1.0453			
49	2	49	<C>				1.0466			
48	4	48	<C>				1.0483			
47.5	5	47.5	R tr. + <C>				1.0484			
45	10	45	R + <C>	0.6083	0.5837	0.8537	1.0484			
30	40	30	R + <C>	0.6023	0.5819	0.8395	1.0497			
29	42	29	R + <C>	0.6029	0.5820	0.8509	1.0464			
27.5	45	27.5	R + <C>	0.6006	0.5820	0.8388	1.0482			
26	48	26	R	0.6044	0.5821	0.8397				
25	50	25	R	0.6007	0.5830	0.8418				
23.5	53	23.5	R	0.6019	0.5842	0.8424				
22.5	55	22.5	<A> + R	0.6022	0.5843	0.8437				
20	60	20	<A> + R	0.6007	0.5844	0.8486	0.6479	0.3813		
7.5	85	7.5	<A> + R	0.6030	0.5851	0.8333	0.6497	0.3816		
5	90	5	<A> + R tr.				0.6507	0.3818		
4	92	4	<A> + R tr.				0.6505	0.3821		
2.5	95	2.5	<A>				0.6517	0.3830		

*) Note that the oxide of lanthanum is subject to hydration in air and, thus, instead of hexagonal A-La₂O₃ in the samples after heat treatment at 1600 °C we found the formation of hexagonal A-La(OH)₃. This arose in this work, however, proper storage and prompt investigation after annealing would have made it possible to obtain A-La₂O₃. Nevertheless, since this applies only to A-La₂O₃ in the investigated system, the results obtained for La(OH)₃ can be attributed to A-La₂O₃. Designation of phases: <A> - solid solutions based on hexagonal modifications of La(OH)₃; <C> - solid solutions based on cubic modification of Lu₂O₃(Er₂O₃); R - ordered phase of LaLuO₃(LaErO₃) with perovskite-type structure with rhombic distortions.

The results were used to construct the isothermal sections of the La₂O₃-Lu₂O₃-Er₂O₃ system at 1500 and 1600 °C (Fig. 1).

Fields of solid solutions based on cubic (C) modifications of Lu₂O₃(Er₂O₃), hexagonal (A) modification of La₂O₃, and ordered perovskite-

type LaLuO₃ and LaErO₃(R) phases form in the La₂O₃-Lu₂O₃-Er₂O₃ system at 1500 and 1600 °C. No new phases were found.

XRD patterns of samples characterizing the phase fields present in the La₂O₃-Lu₂O₃-Er₂O₃ system at 1600 °C are presented in Fig. 2.

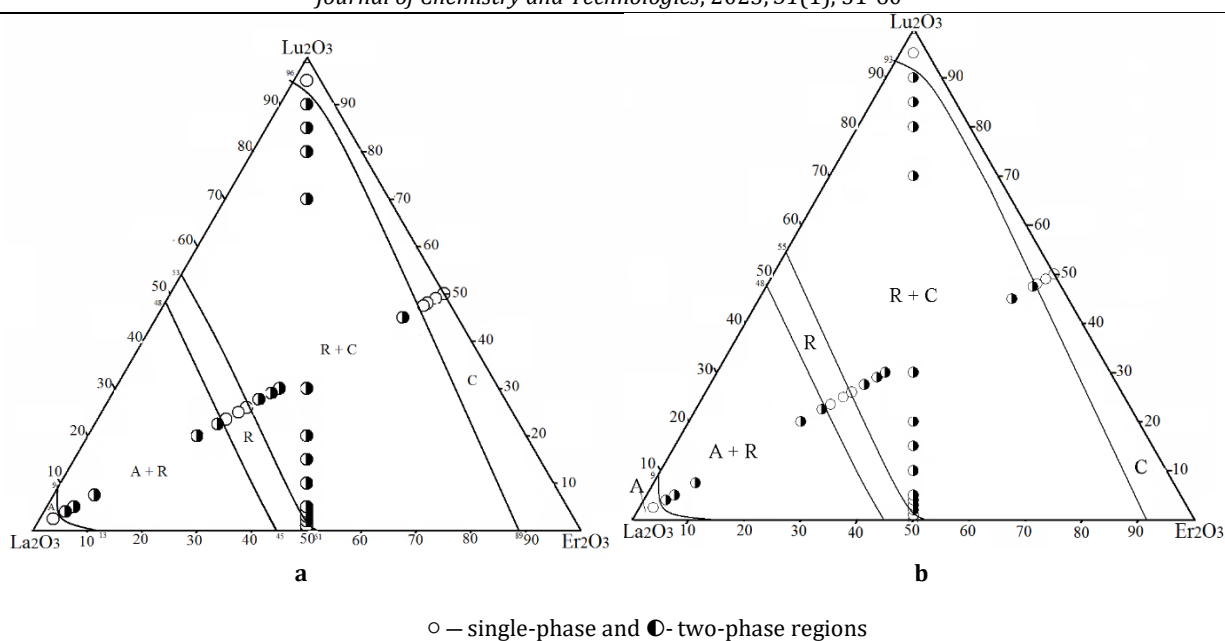
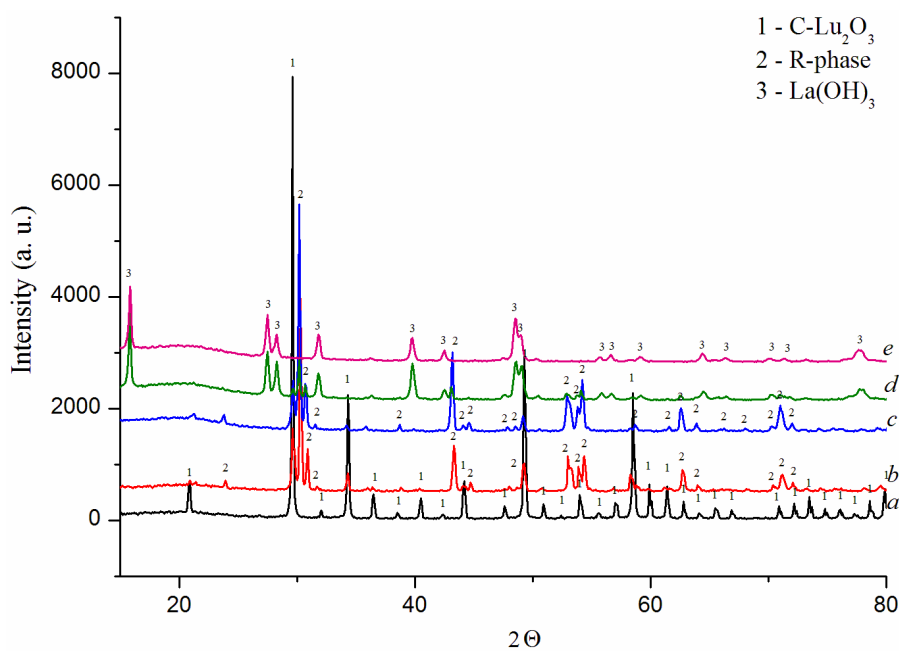


Fig. 1 The isothermal section of the La_2O_3 - Lu_2O_3 - Er_2O_3 phase diagram at 1500 (a) and 1600 (b) °C



a – 49 mol % Lu_2O_3 -2 mol % La_2O_3 -49 mol % Er_2O_3 (C);
b – 29 mol % Lu_2O_3 -42 mol % La_2O_3 -29 mol % Er_2O_3 (C + R);
c – 25 mol % Lu_2O_3 -50 mol % La_2O_3 -25 mol % Er_2O_3 (R);
d – 7,5 mol % Lu_2O_3 -85 mol % La_2O_3 -7,5 mol % Er_2O_3 (R+ A* - $\text{La}(\text{OH})_3$);
e – 2,5 mol % Lu_2O_3 -95 mol % La_2O_3 -2,5 mol % Er_2O_3 (A* - $\text{La}(\text{OH})_3$)

Fig. 2. XRD patterns from the La_2O_3 - Lu_2O_3 - Er_2O_3 samples heat-treated at 1600 °C

A infinite continuous serie area of solid solutions based on ordered perovskite-type phases forms in the La_2O_3 - Lu_2O_3 - Er_2O_3 system. This indicates the mutual substitution of Lu^{3+} ($r = 0.085$ nm) ions by Er^{3+} ($r = 0.881$ nm), and vice versa. Using the concentration dependences of the unit cell parameters, it was established that the range of homogeneity of solid solutions based on the R-phase extends from 46 to 54 mol % La_2O_3 at 1500 °C and from

~48 to 54 mol % La_2O_3 at 1600 °C in the section La_2O_3 - (50 mol % Lu_2O_3 -50 mol % Er_2O_3) (Fig. 3). The lattice parameters of the unit cell R phase vary from $a = 0.609$ nm, $b = 0.585$ nm, $c = 0.842$ nm in the single-phase sample of the composition 1 mol % Lu_2O_3 -49.5 mol % La_2O_3 -49.5 mol % Er_2O_3 to $a = 0.586$ nm, $b = 0.583$ nm, $c = 0.851$ nm in the two-phase (R + C) sample of the composition 2 mol % Lu_2O_3 -49 mol % La_2O_3 -

49 mol % Er₂O₃ in the section Lu₂O₃–(50 mol % La₂O₃–50 mol % Er₂O₃) (1500 °C).

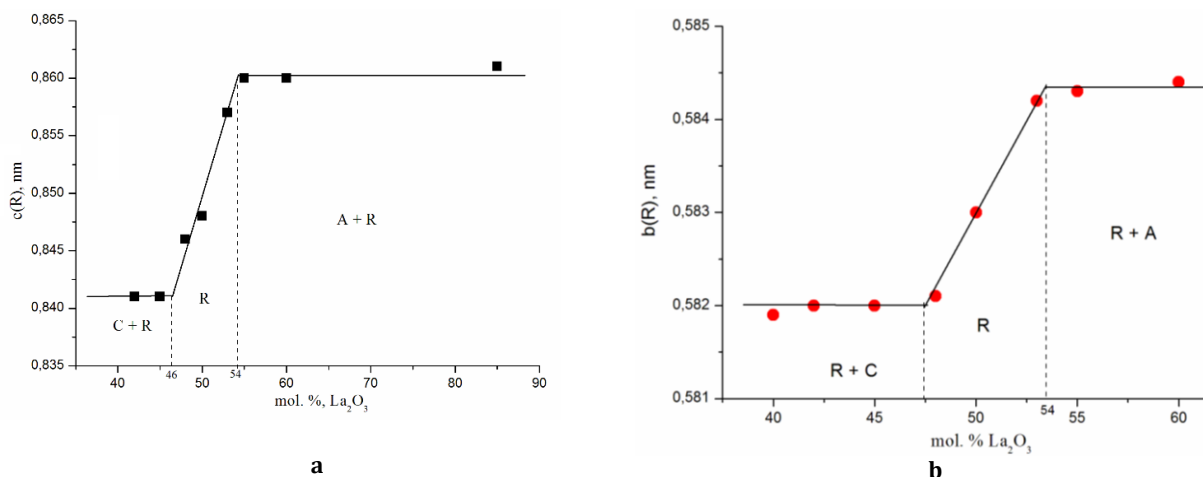


Fig. 3 Concentration dependence of lattice parameters (c and b) for R-based solid solutions annealed at 1500 (a) and 1600 (b) °C along the section Lu₂O₃–(50 mol % Lu₂O₃–50 mol % Er₂O₃) in the system Lu₂O₃–Lu₂O₃–Er₂O₃

Similar to this system, in the Lu₂O₃–Lu₂O₃–Yb₂O₃ [27] and Lu₂O₃–Y₂O₃–Er₂O₃ [28] systems at 1500 °C, continuous series of solid solutions based on an ordered phase with a perovskite-type structure are also formed. In contrast, in the Lu₂O₃–Y₂O₃–Nd₂O₃ system at 1500 °C, a region of solid solutions is formed based on an ordered phase with a perovskite-type structure. The maximum solubility of neodymium oxide in the R phase is ~ 7 mol % along section Nd₂O₃–(50 mol % La₂O₃–50 mol % Y₂O₃) [29].

Lutetium and erbium oxides form a continuous series of C-REE oxide solid solutions. This field ranges along the Lu₂O₃–Er₂O₃ side of the composition triangle. This direction of the

homogeneity range of the C-phase indicates that Lu³⁺ ions are predominantly replaced by Er³⁺ ions and vice versa, without charge compensation. The composition dependence of the lattice parameters shows that the homogeneity range of the C-phase solid solutions extends from 95 to 100 (1500 °C) and ~93 до 100 (1600 °C) mol % Lu₂O₃ at section Lu₂O₃–(50 mol % La₂O₃–50 mol % Er₂O₃) (Fig. 4) and from 0 to 6 (1500 °C) and 0 до 5 (1600 °C) mol % La₂O₃ at section La₂O₃–(50 mol % Lu₂O₃–50 mol % Er₂O₃) (Fig. 5).

For comparison, in the Lu₂O₃–Lu₂O₃–Yb₂O₃ system at 1500 [27] and 1600 [30] °C, a continuous series of solid solutions based on the C-form of REE oxides is also formed.

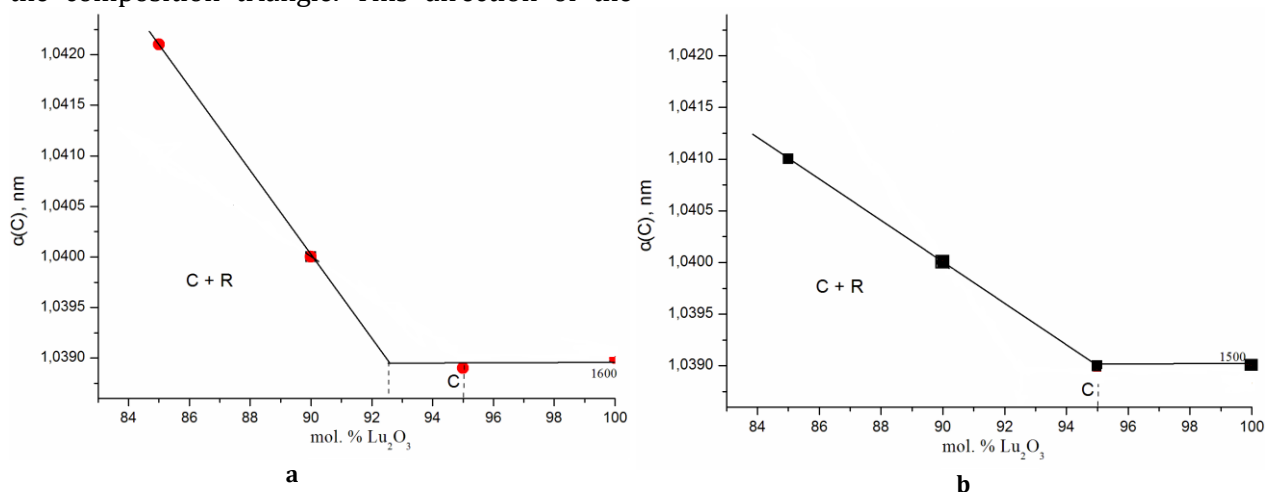


Fig. 4 Concentration dependence of lattice parameters (a) for C-based solid solutions annealed at 1500(a) and 1600(b) °C along the section Lu₂O₃–(50 mol % La₂O₃–50 mol % Er₂O₃) in the system Lu₂O₃–Lu₂O₃–Er₂O₃

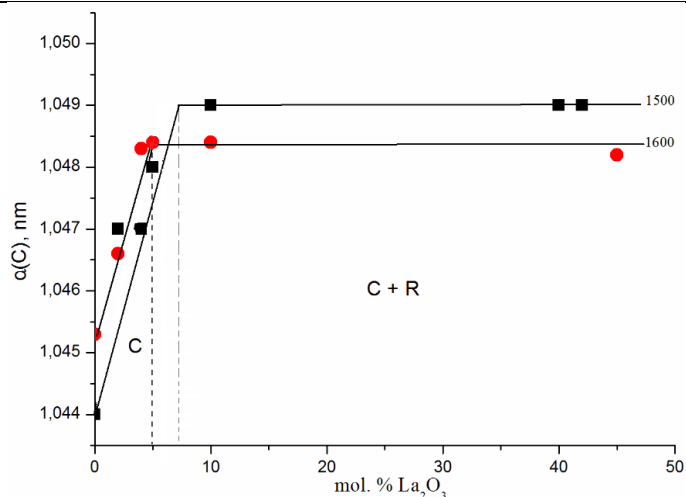


Fig. 5 Concentration dependence of lattice parameters (a) for C-based solid solutions annealed at 1500 and 1600 °C along the section of La_2O_3 –(50 mol % Lu_2O_3 –50 mol % Er_2O_3) in the system La_2O_3 – Lu_2O_3 – Er_2O_3

The homogeneity range of the solid solution based on the hexagonal (A) modification of lanthanum oxide is not extensive wide. Note that the oxide of lanthanum is subject to hydration in air and, thus, instead of hexagonal A- La_2O_3 in the samples after heat treatment at 1500 and 1600 °C we found the formation of hexagonal A- $\text{La}(\text{OH})_3$ (Fig. 2 e, d). This arose in this work, however, proper storage and prompt investigation after annealing would have made it possible to obtain A- La_2O_3 . Nevertheless, since this applies only to A- La_2O_3 in the investigated system, the results obtained for $\text{La}(\text{OH})_3$ can be attributed to A- La_2O_3 . The field of this homogeneity range is concave in the direction of decreasing the content of erbium oxide and extends in accordance with

boundaries in the bounding La_2O_3 – Lu_2O_3 and La_2O_3 – Er_2O_3 binary systems. The composition dependence of the lattice parameters shows that the homogeneity range of the A-phase solid solutions extends from ~94 to 100 (1500 °C) and ~93 to 100 (1600 °C) mol % La_2O_3 at section La_2O_3 –(50 mol % Lu_2O_3 –50 mol % Er_2O_3) (Fig. 6). At 1500 °C, the lattice parameters of the unit cell of A- $\text{La}(\text{OH})_3$ vary from $a = 0.651$ nm, $c = 0.387$ nm in the sample of the composition 2.5 mol % Lu_2O_3 –95 mol % La_2O_3 –2.5 mol % Er_2O_3 , to $a = 0.654$ nm, $c = 0.385$ nm for 1500 °C in the two-phase (A + R) sample of the composition 20 mol % Lu_2O_3 –60 mol % La_2O_3 –20 mol % Er_2O_3 . A similar correlation is at 1600 °C.

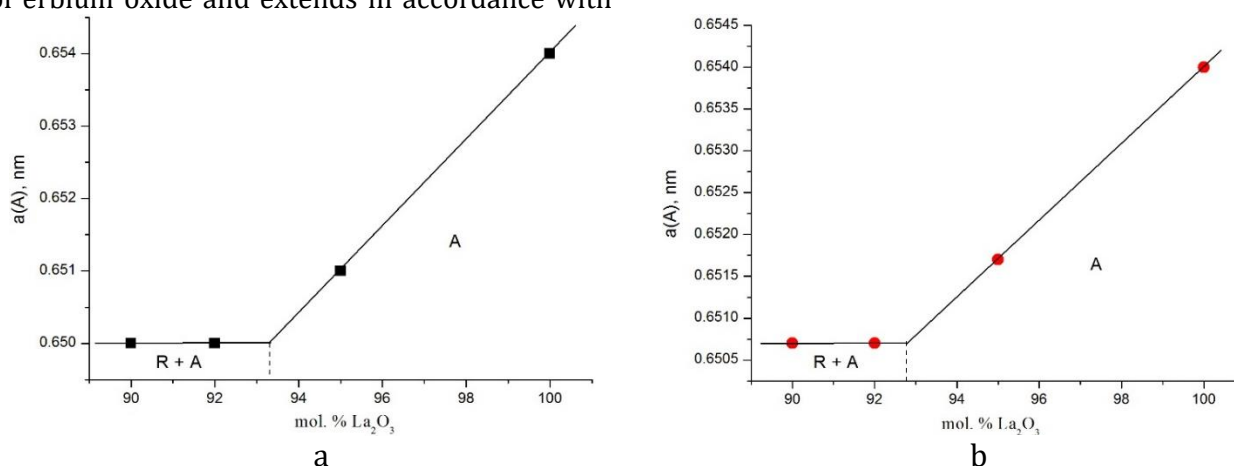
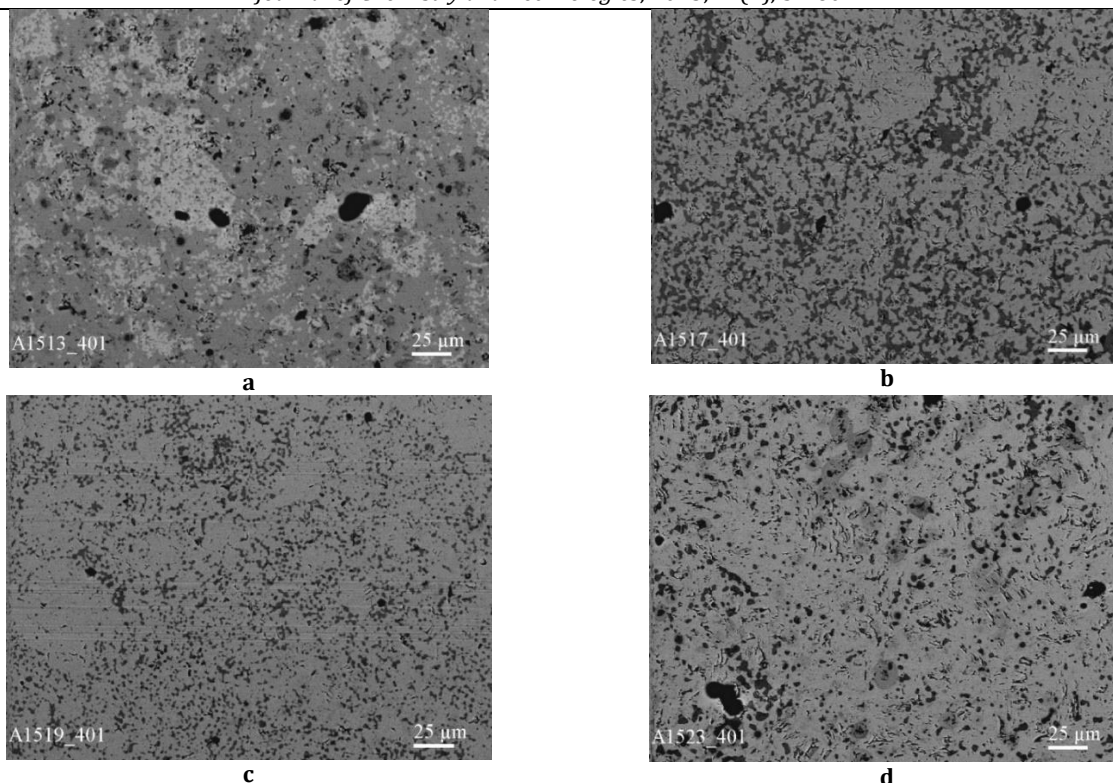


Fig. 6 Concentration dependence of lattice parameters (a) for solid solutions based on A- $\text{La}(\text{OH})_3$ heat-treated at 1500(a) and 1600(b) °C along the section of La_2O_3 –(50 mol % Lu_2O_3 –50 mol % Er_2O_3) in the system La_2O_3 – Lu_2O_3 – Er_2O_3

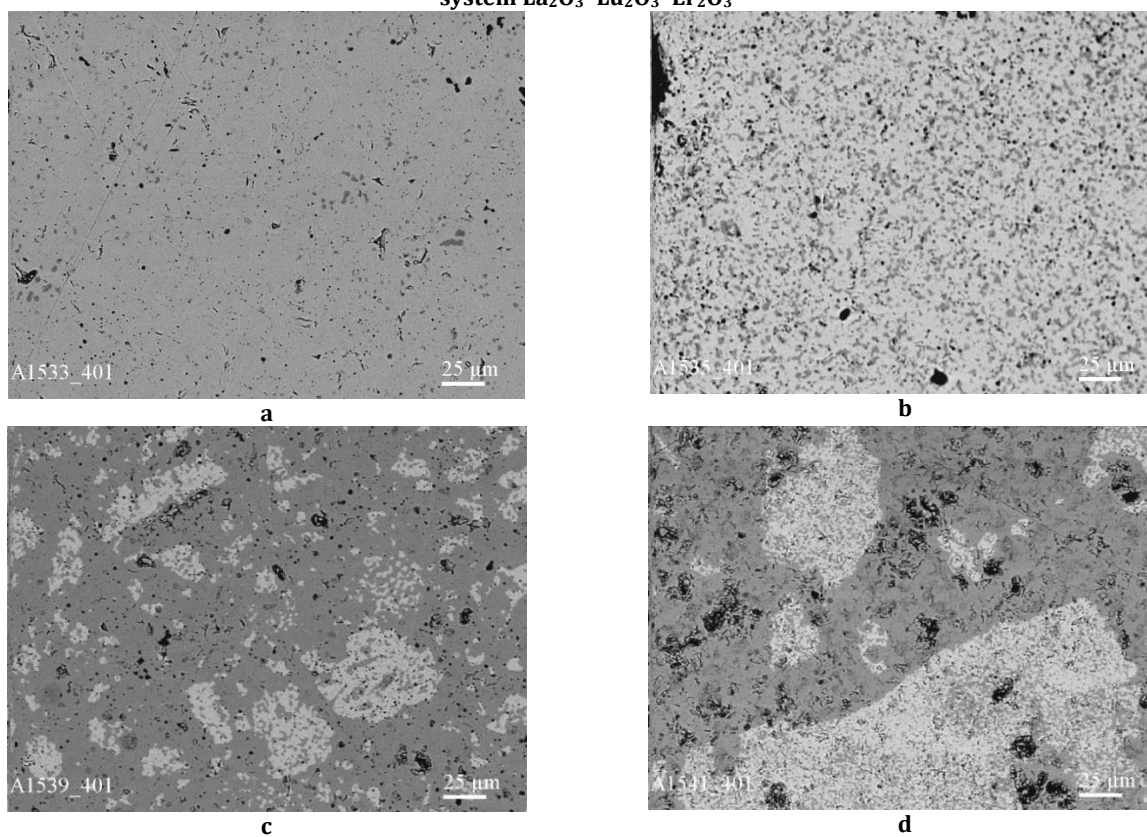
Depending on the lutetium oxide content, microstructural changes in the two-phase samples (C + R) can be followed in Fig. 7 and 8. In fig. 7 shows microstructures of the samples lying on the Lu_2O_3 –(50 mol % La_2O_3 – 50 mol % Er_2O_3) section. In fig. 8 shows microstructures of

samples lying on the La_2O_3 –(50 mol % Lu_2O_3 – 50 mol % Er_2O_3) section. The C phase is light and the R phase is dark. With increasing lutetium oxide content, the amount of the perovskite-type phase decreases (Figs. 7, 8).



a - 15 mol % Lu_2O_3 -42,5 mol % La_2O_3 -42,5 mol % Er_2O_3 (R + C); *b* - 70 mol % Lu_2O_3 -15 mol % La_2O_3 -15 mol % Er_2O_3 (R + C); *c* - 80 mol % Lu_2O_3 -10 mol % La_2O_3 -10 mol % Er_2O_3 (R + C); *d* - 90 mol % Lu_2O_3 -5 mol % La_2O_3 -5 mol % Er_2O_3 , (R + C). Light phase - C, dark phase - R, black - pores.

Fig. 7. SEM microstructures of the samples heat-treated at 1500 °C in the definite field of compositions of the system La_2O_3 - Lu_2O_3 - Er_2O_3



a - 47.5 mol % Lu_2O_3 -5 mol % La_2O_3 -47.5 mol % Er_2O_3 (R + C); *b* - 45 mol % Lu_2O_3 -10 mol % La_2O_3 -45 mol % Er_2O_3 (R + C); *c* - 29 mol % Lu_2O_3 -42 mol % La_2O_3 -29 mol % Er_2O_3 (R + C); *d* - 27,5 mol % Lu_2O_3 -45 mol % La_2O_3 -27,5 mol % Er_2O_3 , (R + C). Light phase - C, dark phase - R, black - pores.

Fig. 8. SEM microstructures of the samples heat-treated at 1600 °C in the definite field of compositions of the system La_2O_3 - Lu_2O_3 - Er_2O_3

Conclusions

Phase equilibria have been studied in the $\text{La}_2\text{O}_3\text{-Lu}_2\text{O}_3\text{-Er}_2\text{O}_3$ system at 1500 and 1600 °C. It has been established that solid state interactions between three oxides resulted in the formation of extended fields of solid solutions based on various crystal modifications of the initial components of rare-earth oxides, as well as the ordered phase of perovskite type. The isothermal section of the $\text{La}_2\text{O}_3\text{-Lu}_2\text{O}_3\text{-Er}_2\text{O}_3$

phase diagram at 1500 and 1600 °C has characterized the three one-phase fields (A- La_2O_3 , R, C- $\text{Lu}_2\text{O}_3(\text{Er}_2\text{O}_3)$) corresponding to solid solutions based on starting components and two two-phase fields (C + R, A + R) between them.

Acknowledgment

The research effort was funded by NATO (Grant G 5769, Science for Peace and Security Program).

References

- [1] Zatsopin, A., Kuznetsova, Y., Spallino, L., Pustovarov, V., Rychkov, V. (2016) Photosensitive defects in Gd_2O_3 – advanced material for solar energy conversion, *Energy Procedia*, 102, 144–151. <https://doi.org/10.1016/j.egypro.2016.11.329>.
- [2] Wang, S.F., Zhang, J., Luo, D. W., Gu, F., Tang, D. Y., Dong, Z. L., Que, W. X., Zhang, T. S., Li, S., Kong, L.B. (2013). Transparent ceramics: Processing, materials and applications, *Prog. Solid State Chem.*, 41, 20–54. <https://doi.org/10.1016/j.progsolidstchem.2012.12.002>
- [3] Sanghera, J., Bayya, S., Villalobos, G., Kim, W., Frantz, J., Shaw, B., Sadowski, B., Miklos, R., Baker, C., Hunt, M., Aggarwal, I., Kung, F. (2011). Transparent ceramics for high-energy laser systems, *Opt. Mater.*, 33, 511–518. <https://doi.org/10.1016/j.optmat.2010.10.038>
- [4] Chen, B. S., Yiquan, W. (2013). New opportunities for transparent ceramics, *Amer. Ceram. Soc. Bull.*, 2, 32–37.
- [5] Akiyama, J., Sato, Y., Taira, T. (2010). Laser ceramics with rare-earth-doped anisotropic materials, *Optics Lett.*, 35, 3598–3600. <https://doi.org/10.1364/OL.35.003598>
- [6] Taira T. (2011). Domain-controlled laser ceramics toward Giant Micro-photonics, *Opt. Mater. Express.*, 1, 1040–1050. <https://doi.org/10.1364/OME.1.001040>
- [7] Qiu-Hong Yang, Hong-Xu Zhou, Jun Xu, Liang-Bi Su. (2008). Synthesis and luminescence characterization of cerium doped $\text{Lu}_2\text{O}_3\text{-Y}_2\text{O}_3\text{-La}_2\text{O}_3$ solid solution transparent ceramics, *Optics express.*, 16, 12295. [doi:10.1364/oe.16.012290](https://doi.org/10.1364/oe.16.012290).
- [8] Chen, Y., Lin, X., Lin, Y., Luo, Z. (2004). Spectroscopic properties of Yb^{3+} ions in $\text{La}_2(\text{WO}_4)_3$ crystal, *Solid State Communications*, 132, 533–538.
- [9] Gong, X., Xiong, F., Lin, Y. (2007). Crystal growth and spectral properties of $\text{Pr}^{3+}:\text{La}_2(\text{WO}_4)_3$, *Materials Research Bulletin*, 42 413–419.
- [10] Lakshminarasimhan, N., Varadaraju, U. V. (2006). Luminescent host lattices, LaInO_3 and LaGaO_3 —A reinvestigation of luminescence of d10 metal ions, *Materials Research Bulletin*, 41, 724–731.
- [11] Muller-Buschbaum, Hk., Graebner, P. H. (1971). Zur Kristallstruktur von LaErO_3 und LaLuO_3 , *Z. Anorg. Allg. Chem.*, 386, 158–162 (in German).
- [12] Xiong, K., Robertson, J. (2009). Electronic structure of oxygen vacancies in La_2O_3 , Lu_2O_3 and LaLuO_3 , *Microelectr. En.*, 86(7-9), 1672–1675. <https://doi.org/10.1016/j.mee.2009.03.016>
- [13] Chudinovych, O. V., Zhdanyuk, N.V. (2020). Interaction of lanthanum oxides and lutetium at a temperature of 1500–1600 °C, *Ukrainian Chem. J.*, 86(3), 19–25. (in Ukrainian). <https://doi.org/10.33609/0041-6045.86.3.2020.19-25>
- [14] Kornienko, O.A., Chudinovych, O.V., Bykov, A.I., Samelyuk, A.V., Andrievskaya, E.R. (2019). Phase equilibria in the $\text{La}_2\text{O}_3\text{-Er}_2\text{O}_3$ system in the temperature range 1100–1500°C, *Powder Metall. Met. Ceram.*, 58 (1–2), 89–98. <https://doi.org/10.1007/s11106-019-00051-6>.
- [15] Schneider, S.I., Roth, R.S. (1960). Phase equilibria in systems involving the rare-earth oxides. Part II: solid state reactions in trivalent rare-earth oxide systems, *J. of Res. National Bureau Standards. A: Physics and Chem.*, 64 (4), 317–332.
- [16] Foex, M., Traverse, J.P. (1966). Étude du polymorphisme des sesquioxydes de terres rares à haute température, *Bulletin de Minéralogie.*, 89(2), 184–205.
- [17] Coutures, J., Rouanet, A., Verges, R., Foex, M. (1976). Etude à haute température des systèmes formés par le sesquioxyde de lanthane et les sesquioxydes de lanthanides. I: dia-grammes de phases ($1400\text{ °C} < T < \text{Tl}(\text{liquide})$), *J. Solid State Chem.*, 17(1–2), 172–182.
- [18] Zinkevich, Matvei (2007). Thermodynamics of rare earth sesquioxides, *Prog. Mater. Sci.*, 52, 597–647.
- [19] Zhang, Y. (2016). Thermodynamic Properties of Rare Earth Sesquioxides, McGill University, Montreal, QC, Canada), 151.
- [20] Lopato, L.M., Shevchenko, A.V., Kushchevskii, A.V., Tresvyatskii, S.G. (1974). Polymorphic transformations of rare earth oxides at high temperatures, *Izv. AN SSSR. Neorg. Mater.*, 10(8), 1481–1487.
- [21] Traverse, J.P. (1971). Etude du Polymorphisme des sesquioxydes de terres rares. *These. Grenoble*.
- [22] Andrievskaya, E. R. (2010). [Phase equilibria in the systems of hafnium, zirconium and yttrium oxides of rare earth elements], *Naukova dumka, Kiev.* (in Russian).
- [23] Shannon, R. D. (1976). Revised effective ionic radii systematic studies of interatomic distances in halides and chalcogenides, *Acta Crystallogr. A.*, 32, 751–754.
- [24] Zinkevich, M. (2007). Thermodynamic Database for Rare Earth Sesquioxides, <https://materialsdata.nist.gov/handle/11256/965>.
- [25] Pavlik, A., Ushakov, S.V., Navrotsky, A., Benmore, C. J., Weber, R.J.K. (2017). Structure and thermal expansion of Lu_2O_3 and Yb_2O_3 up to the melting points, *J. Nucl. Mater.*, 495, 385–391.
- [26] Axelrud, L.G., Grin, Yu. N., Zavaliy, P. Yu. (1990). Software Package for Structural Analysis of Crystals, *CSD, General description, Lviv*.
- [27] Chudinovych, O. V., Bykov, O. I., Sameliuk, A.V. (2021). Phase relation studies in the $\text{La}_2\text{O}_3\text{-Lu}_2\text{O}_3\text{-Yb}_2\text{O}_3$ system at 1500 °C, *Journal of Chemistry and Technologies*, 29(4), 485–494.
- [28] Chudinovych, O. V., Bykov, O. I. (2020). Interaction of yttrium, lanthanum and erbium oxides at the

- temperature of 1500°C, *Voprosy Khimii i Khimicheskoi Tekhnologii*, 4, 194-200.
- [29] Chudinovich, O. V., Andrievskaya, O. R., Bogatyryova, J. D., Kovylyaev, V. V., Bykov, O. I. (2021). Phase equilibria in the $\text{La}_2\text{O}_3\text{-Y}_2\text{O}_3\text{-Nd}_2\text{O}_3$ system at 1500 °C, *J. Eur. Ceram. Soc.*, 41, 6606–6616.
<https://doi.org/10.1016/j.jeurceramsoc.2021.06.017>
- [30] Chudinovich, O. V., Bykov, O. I., Sameliuk, A.V. (2021). Interaction of lanthanum, lutetium, and ytterbium oxides at 1600 °C, *Powder Metallurgy and Metal Ceramics*, 60(5-6), 337–346.
<https://doi.org/10.1007/s11106-021-00248-8>